CFD Simulation of Flow over NACA 0012 Airfoil

Tejasvi Singh, Gaurav Mittal, Sanchit Mittal and Riya Tyagi

May 21, 2022

CFD Simulation of Flow Over NACA 0012 Airfoil

Tejasvi Singh[1, a)], Gaurav Mittal[1, b)], Sanchit Mittal[1, c)], and Riya Tyagi[1, d)]

[1]*Department of Mechanical Engineering, Graphic Era Deemed to be University, Dehradun, UK, India*

a) singhtejasvi1122@gmail.com
b) Corresponding author: gauravmittal@geu.ac.in
c) sanchitmital7@gmail.com
d) riyatyagi1013@gmail.com

Abstract. Fluid flow over a NACA airfoil (NACA 0012) was simulated using ANSYS FLUENT. A two-dimensional steady state simulation was conducted along with SST k- ω turbulence model. Grid independency was established and study was done by varying Reynolds number and angle of attack over a range of 5x10^5 to 2x10^6 and -15^o to 15^o, respectively. Lift and drag coefficients were calculated from the simulations and compared with their experimental values. An excellent agreement was noted for the coefficient of lift. However, some discrepancies were observed and highlighted for the coefficient of drag. Specifically, the simulated values of drag coefficients were 30 to 100% higher than the experimental values. The discrepancies are attributed to the selection of turbulence model and 2-D steady state flow. Over the range of parametric variation in this study, both lift and drag coefficients increased with an increase in the angle of attack. The effect of variation in Reynolds number was minor. The coefficient of drag decreased with Reynolds number, whereas the coefficient of lift remained almost unchanged.

INTRODUCTION

Aerodynamic forces on airfoils play an important role for aircraft wings, propellers, wind turbines etc [1]–[4]. These forces are typically resolved into a lift and a drag force. Particularly, a number of researchers have studied NACA airfoils [1], [3], [5]–[7]. NACA stands for 'National Advisory Committee for Aeronautics'. During the late 1920s, NACA developed a family of airfoils, such as NACA 4412, NACA 0012, NACA 2415. All airfoils were thoroughly tested in wind tunnels under different practical conditions.

Along with the experiments, it is also very important to investigate aerodynamics of airfoils computationally and have predictive capabilities [8], [9]. Sadikin et al. [1] in their study analysed CFD simulation past a 2D NACA 0012 airfoil at Reynolds number of 3x10^6 for angles of attack -10^o to 15^o. They used various turbulence models and noted that the realizable $k-\epsilon$ model results in elimination of the separation bubble on airfoil, whereas the SST $k-\omega$ model predicted a separation bubble. They provided some guidance regarding optimum turbulence model for simulation. Patel et el. [10] simulated 2D subsonic flow over NACA 0012 airfoil over a range of angle of attacks at constant Reynolds number. Yilmaz et al. [6] compared results obtained by CFD simulation of NACA 0012 and NACA 4412 airfoils for various angles of attack with constant Reynolds number of 10^6. They evaluated the influence of asymmetry in airfoil profile and discussed optimum angle of attack for each airfoil which gives maximum ratio of the coefficient of lift and drag.

AlMutairi et al. [11] used LES to study the dynamics of laminar separation bubble for NACA 0012 airfoil near conditions of stall. A low frequency flow oscillation was noted by them and the simulated values of Strouhal number matched well with the experimental data. Zhou et al. [12] investigated the control of flow separation for NACA 4405. They observed that the placement of a plate near the leading edge of the airfoil can be effective in delaying the separation of flow.

In this work, NACA 0012 airfoil has been selected for study. For simulating the air flow, ANSYS FLUENT is used in conjunction with the SST $k-\omega$ turbulence model. This turbulence model is employed extensively in aerodynamic simulation. Following the computations, the simulated lift and drag coefficients are compared with the actual data available on the NACA website. The specific objective of this work is to evaluate the predictive capability of the chosen turbulence model under the conditions investigated in this work.

COMPUTATIONAL SPECIFICATIONS

The geometry of NACA 0012 airfoil is shown in Fig. 1. In the NACA four-number wing section description, the first number stands for the maximum camber in terms of percent of the chord length, the second number stands for the distance between the maximum camber point and the leading edge of the airfoil in tenths of the chord and the last two numbers stand for the maximum thickness of the airfoil in terms of percent of the chord. NACA 0012 airfoil is symmetrical; the first two digits as 00 indicate zero camber. Last two digits, as 12, indicate that the thickness of the airfoil is 12% of the chord length.

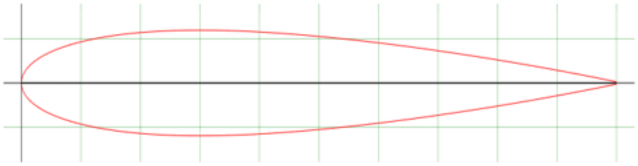

FIGURE 1. Geometry of NACA 0012 airfoil

The computational domain is shown in Fig. 2. The chord length of airfoil was taken as 1 m. The radius of the front semi-circular portion was 20 m. The domain thus had a height of 40 m and it extended for 30 m behind the airfoil in the wake region. A large domain was taken because boundary conditions of velocity and pressure at location far from the airfoil, which are free stream velocity and atmospheric pressure, can be specified with confidence.

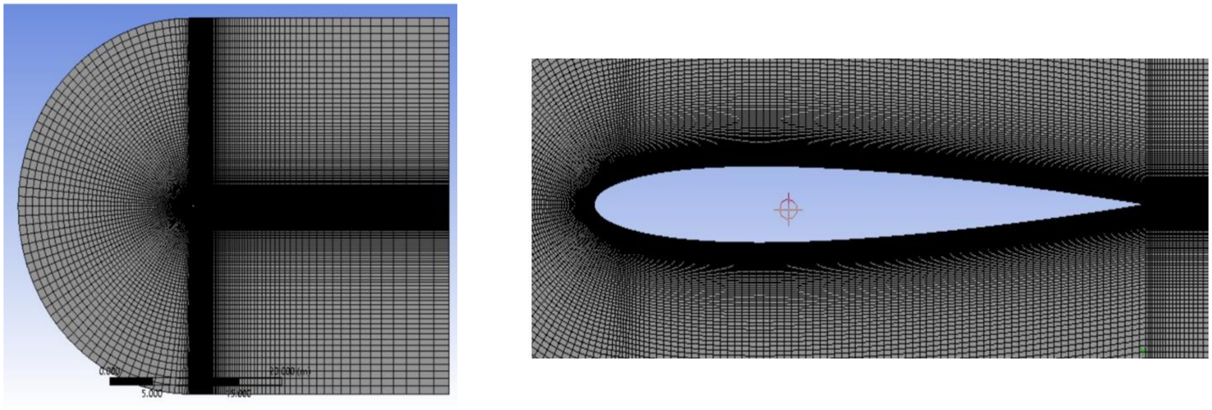

(a) (b)

FIGURE 2. (a) Entire **c**omputational domain along with mesh. (b) Enlarged view of the airfoil

A structured mesh was generated with a fine grid distribution near the airfoil wall and coarser in the region away from the airfoil. The sizing method with biasing feature was used to obtain such mesh. The grid distribution is shown in Fig. 2. Pressure-based solver was used with SIMPLE algorithm and second order upwind differencing for the convective term. The SST- k- ω turbulence model was used. This is a two-equation eddy-viscosity model. It is amalgamation of two models k- ω and k-ε. The k-ω model is appropriate for simulating flow in viscous layer, like near the airfoil wall whereas the k- ε model is used for predicting flow behaviour in region distant from the wall. Air at 300K and 1 atm was used as the fluid considering it an ideal gas with constant viscosity.

RESULTS

Grid independency was conducted to ensure that the solution is not very much affected by using finer grid. The pressure field for Reynolds number of $2x10^6$ for various grid distributions are shown in Fig. 3. The upper surface entails lower pressure, whereas higher pressure is noted on the lower surface. The simulations were done with approximately 70000, 140000 and 280000 cells.

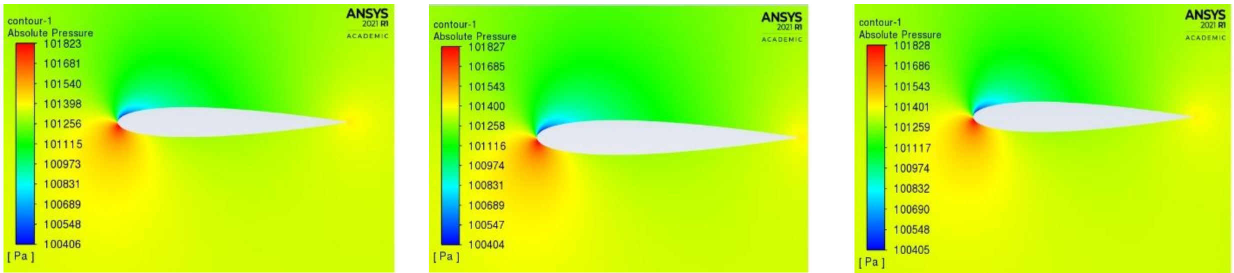

(a) (b) (c)

FIGURE 3. Pressure distribution for (a) coarse (b) medium and (c) fine grid. Re = $2x10^6$, angle of attack = 5^o

The lift and drag coefficients, normalized by the fine grid value, are plotted in Fig. 4 and demonstrate grid independence. Sample streamlines, velocity and pressure field for an angle of attack = 5^o and Re = $2x10^6$ are shown in Fig. 5. The stagnation point and flow acceleration above the airfoil can be clearly noted.

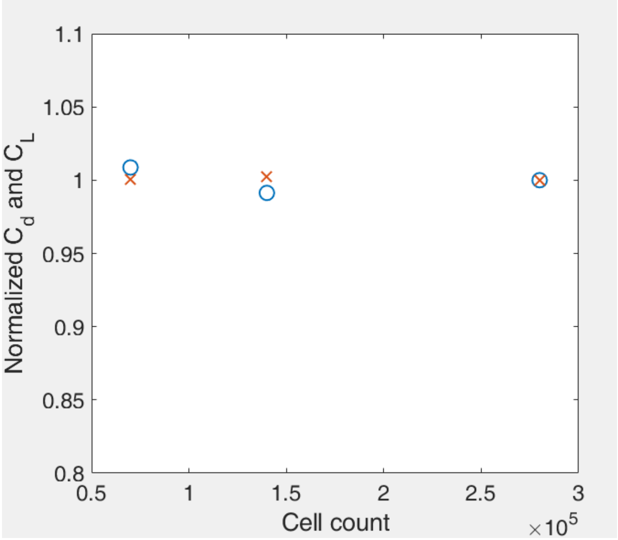

FIGURE 4. Normalized C_d and C_L vs cell count. Re = $2x10^6$, angle of attack = 5^o

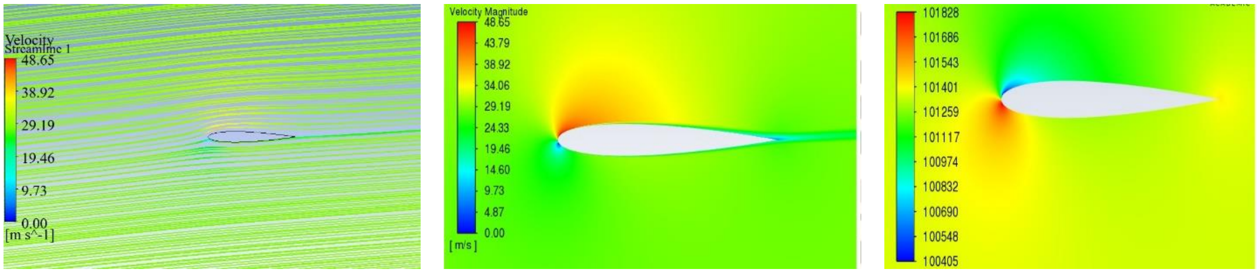

(a) (b) (c)

FIGURE 5. (a) streamlines (b) velocity and (c) absolute pressure (in Pa). Re = $2x10^6$, angle of attack = 5^o

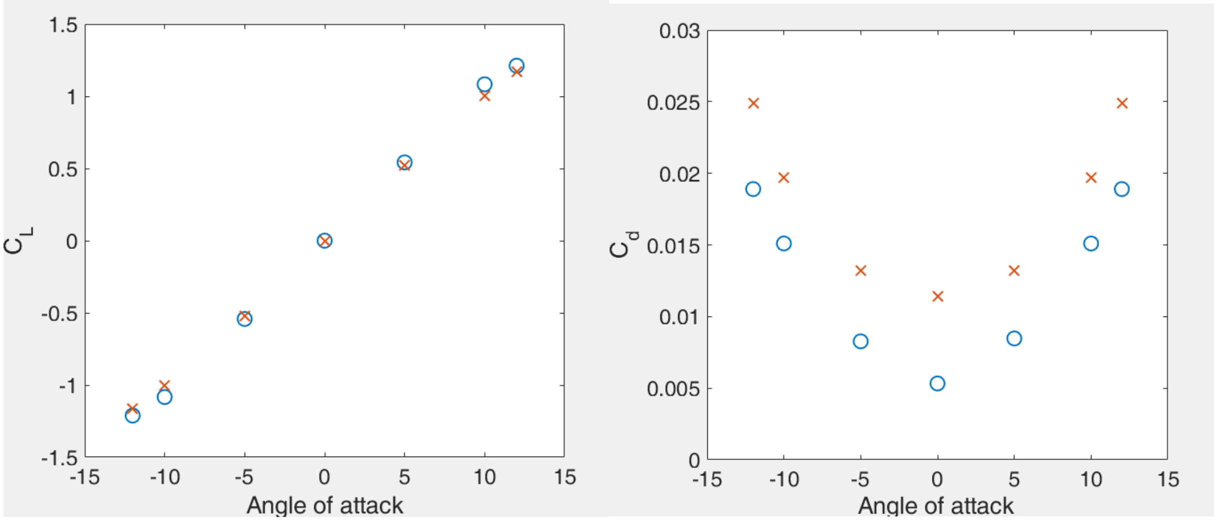

FIGURE 6. Experimental (circle) and simulated (cross) C_d and C_L . Re = 1x10^{6}

Simulations were conducted over a range of angle of attack for Reynolds number of 1x10^{6}. A comparison of the simulated and experimental lift and drag coefficients is shown in Fig. 6. For the angles of attack studied here, the variation of coefficient of lift is pretty linear. This linear trend is not expected to continue at higher angles of attack due to impending flow separation. The agreement with experiments for the lift coefficient is remarkable. However, discrepancy can be seen in the drag coefficients even though the trend is well captured. The simulated values of drag coefficient are 30 to 100% higher than the experimental values. The discrepancy is lower at higher angles of attack. The ratio of lift and drag coefficients is plotted in Fig. 7. Both the lift and drag coefficients increase with angle of attack; however, the lift coefficient increases more than the drag coefficient, thus resulting in a high C_L/C_D ratio. Again, the simulated results capture the trend but the simulated ratios are somewhat lower.

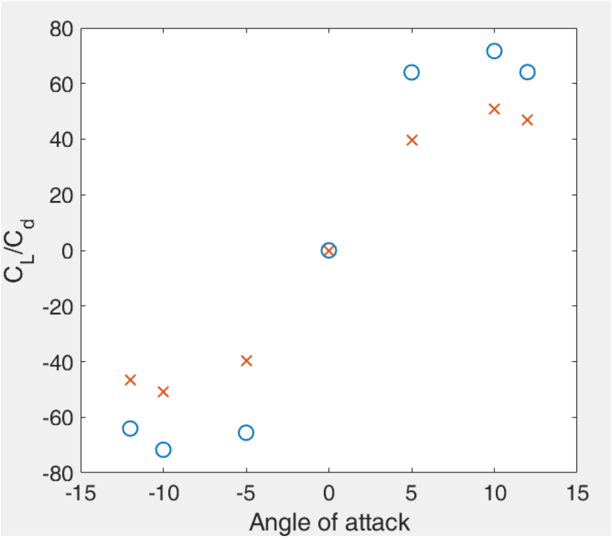

FIGURE 7. Experimental (circle) and simulated (cross) $C_L/\ C_d$. Re = 1x10^{6}

Further simulations were conducted by varying Reynolds number while keeping the angle of attack fixed at 5°. The experimental as well as simulated results are shown in Fig. 8. The variation in the coefficient of lift over the selected Reynolds number range is small and simulated results do not differ significantly from the experiments. Nonetheless, the drag coefficients are overpredicted by about 45% by the simulations, but the decreasing trend of drag coefficient with Reynolds number is well captured.

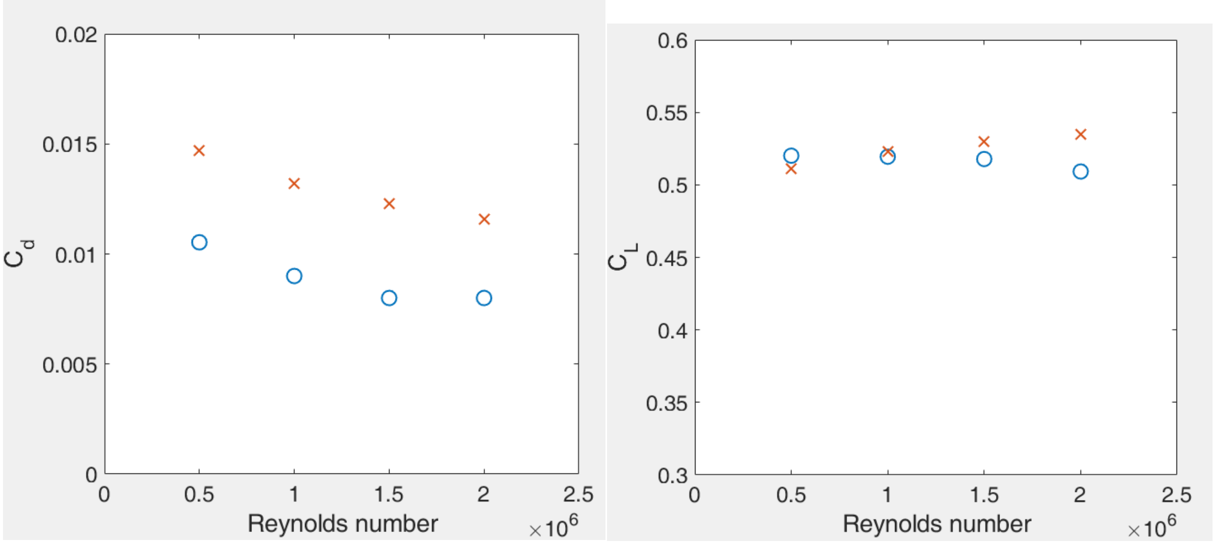

FIGURE 8. Experimental (circle) and simulated (cross) C_d and C_L . Angle of attack = 5°

CONCLUSION

Study of flow over airfoils is crucial for applications involving wind turbines, helicopter rotors, aircraft wings etc. In this work, flow over NACA 0012 was simulated using ANSYS FLUENT. Specifically, the performance of the SST k- ω turbulence model was assessed by comparing experimental and simulated lift and drag coefficients. The SST k- ω turbulence model did an excellent job in capturing the coefficient of lift and the trends in the coefficient of drag. However, it always overpredicted the drag coefficients.

REFERENCES

[1] A. Sadikin *et al.*, "A comparative study of turbulence models on aerodynamics characteristics of a NACA0012 airfoil," *Int. J. Integr. Eng.*, vol. 10, no. 1, 2018.

[2] C. Tarhan and Ilker Yilmaz, "Numerical and experimental investigations of 14 different small wind turbine airfoils for 3 different reynolds number conditions," *Wind Struct.*, vol. 28, no. 3, pp. 141–153, 2019.

[3] A. Seeni and P. Rajendran, "Numerical validation of NACA 0009 airfoil in ultra-low reynolds number flows," *Int. Rev. Aerosp. Eng.*, vol. 12, no. 2, pp. 83–92, 2019.

[4] O. Erkan, M. Özkan, T. H. Karakoç, S. J. Garrett, and P. J. Thomas, "Investigation of aerodynamic performance characteristics of a wind-turbine-blade profile using the finite-volume method," *Renew. Energy*, vol. 161, pp. 1359–1367, 2020.

[5] R. I. Rubel, M. K. Uddin, M. Z. Islam, and M. D. Rokunuzzaman, "Numerical and experimental investigation of aerodynamics characteristics of NACA 0015 aerofoil," *Int. J. Eng. Technol. IJET*, vol. 2, no. 4, pp. 132–141, 2016.

[6] M. Yilmaz, H. Koten, E. Çetinkaya, and Z. Co\csar, "A comparative CFD analysis of NACA0012 and NACA4412 airfoils," *J. Energy Syst.*, vol. 2, no. 4, pp. 145–159, 2018.

[7] O. Gunel, E. Koç, and T. Yavuz, "Comparison of CFD and Xfoil airfoil analyses for low Reynolds number," *Int. J. Energy Appl. Technol.*, vol. 3, no. 2, pp. 83–86, 2016.

[8] M. M. M. Saad, S. Bin Mohd, M. F. Zulkafli, and W. M. E. Shibani, "Numerical analysis for comparison of aerodynamic characteristics of six airfoils," in *AIP Conference Proceedings*, 2017, vol. 1831, no. 1, p. 20004.

[9] E. Basta, M. Ghommem, L. Romdhane, and A. Abdelkefi, "Modeling and experimental comparative analysis on the performance of small-scale wind turbines," *Wind Struct.*, vol. 30, no. 3, pp. 261–273, 2020.

[10] K. S. Patel, S. B. Patel, U. B. Patel, and A. P. Ahuja, "CFD Analysis of an Aerofoil," *Int. J. Eng. Res.*, vol.

3, no. 3, pp. 154–158, 2014.

[11] J. AlMutairi, E. ElJack, and I. AlQadi, “Dynamics of laminar separation bubble over NACA-0012 airfoil near stall conditions,” *Aerosp. Sci. Technol.*, vol. 68, pp. 193–203, 2017.

[12] Y. Zhou, L. Hou, and D. Huang, “The effects of Mach number on the flow separation control of airfoil with a small plate near the leading edge,” *Comput. \& Fluids*, vol. 156, pp. 274–282, 2017.